Monatshefte für Chemie - Chemical Monthly
https://doi.org/10.1007/s00706-019-02545-w

ORIGINAL PAPER

Halo-heterocyclization of butenyl(prenyl)thioethers of 4,5-diphenyl-1,2,4-triazol-3-thiole into triazolo[5,1-*b*] [1,3]-thiazinium systems: experimental and theoretical evolution

Nataliya Korol[1] · Mikhail Slivka[1] · Maksym Fizer[1] · Vjacheslav Baumer[2] · Vasyl Lendel[1]

Received: 12 October 2019 / Accepted: 27 December 2019

Abstract

A facile and highly efficient regioselective synthesis of partially saturated triazolo[5,1-*b*][1,3]thiazinium salts by the electrophilic heterocyclization of the butenyl thioethers of 4,5-diphenyl-1,2,4-triazol-3-thiol with halogens was developed. Under developed conditions, electrophilic cyclization reactions proceeded smoothly and cleanly and the corresponding fused products were obtained in high yields in all cases examined. Herein, we also report the studying of the regiochemistry of this process using computer simulation methods, XDR, and spectral investigations for explaining of electrophilic cyclization mechanism and solving of final products structure.

Graphic abstract

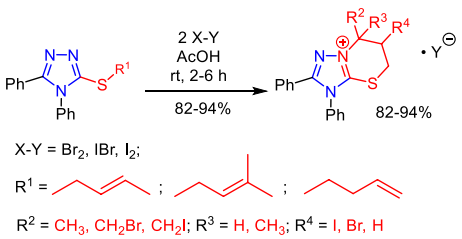

Keywords Regioselectivity · Electrophilic heterocyclization · Butenyl thioethers · Mechanism · Computer simulation methods

Introduction

Triazolo[5,1-*b*][1,3]thiazines have attracted considerable attention because of the availability of synthesis [1–5] and their high pharmacological effects [6–8]. Herein, we have used the method of electrophilic heterocyclization, which became indispensable for the synthesis of the broad range of fused heterocycles [9–23].

In our previous work, we have established that electrophilic heterocyclization of propenyl and propargyl thioethers of 1,2,4-triazole in acetic acid leads regioselectively to annelation of a five- or six-membered ring, depending on the nature of the unsaturated fragment [5, 24–26]. However, D. Kim and co-authors have described the decreasing of the regioselectivity using non-polar solvents [27]. In addition, they have noted the high regioselectivity of iodination of alkenyl thioethers with the introduction of triflouromethyl substituent at the C(5) of triazole ring [28]. We have continued to study the impact of nature of alkenyl moiety on the regiochemistry of electrophilic cyclization. Herein, we wish to report about highly efficient regioselective synthesis

Electronic supplementary material The online version of this article (https://doi.org/10.1007/s00706-019-02545-w) contains supplementary material, which is available to authorized users.

✉ Nataliya Korol
nataliya.korol@uzhnu.edu.ua

[1] Organic Synthesis Laboratory, Uzhhorod National University, Uzhhorod 88000, Ukraine

[2] SSI "Institute for Single Crystals" NASU, Nauky ave. 60, Kharkiv 61001, Ukraine

Published online: 31 January 2020

of triazolo[5,1-*b*][1,3]thiazinium salts by the electrophilic heterocyclization of the butenyl thioethers of 4,5-diphenyl-1,2,4-triazol-3-thiol with halogens, as well as about the studying of the regiochemistry of this process using computer simulation methods and spectral investigations.

Results and discussion

General synthetic methodology

To begin our initial investigation, three unsaturated thioethers **2a**–**2c** were first synthesized to evaluate their ability to promote the regioselective electrophilic cyclization under the action of halogens loading at room temperature in AcOH (Scheme 1). The optimal scale for the production of starting butenyl derivatives **2a**–**2c** was to the usage of 10 mmol of triazole **1**, 12 mmol of a base and 12 mmol of corresponding alkenyl bromide at refluxing in ethanol during 1 h. After cooling to room temperature, the solid products were filtered off, washed with deionized water, dried, and purified by crystallization from ethanol. This procedure turned out to be sufficient to obtain the desired products with high spectroscopic and analytical purity.

The electrophilic halocyclization of received thioethers **3a**–**3c** was performed in different solvents at constant stirring, room temperature, and two-fold excess of halogen (Scheme 1). We have found that a substantial change of the solvent has a significant effect on the halocyclization. Among the solvents tested, the glacial acetic acid appeared to be the most suitable reaction medium, giving the product with 84–89% yield (Table 1, entries 1, 6, 7). Despite the fact that MeCN slightly reduces the reaction yields (down to 86% and 80% for the bromination and iodination, respectively, entries 2, 8), it is an interesting alternative for the glacial acetic acid, especially when starting thioether also contains amine moiety [19]. Screening of solvents reveal that more polar solvents offered a better yield then less polar. The lower results were obtained when tetrachloromethane was employed (Table 1, entries 5, 11).

Table 1 Impact of solvent on cyclization of thioether **2a**–**3a**

Entry	Electrophile	Solvent	Yield/%
1	Br_2	CH_3COOH	89
2	Br_2	CH_3CN	86
3	Br_2	CCl_4	54
4	Br_2	$CHCl_3$	67
5	Br_2	CH_2Cl_2	58
6	IBr	CH_3COOH	84
7	I_2	CH_3COOH	85
8	I_2	CH_3CN	80
9	I_2	CCl_4	70
10	I_2	$CHCl_3$	74
11	I_2	CH_2Cl_3	70
12	I_2	C_2H_5OH	81

Structural investigations

The indicated model 3-*R*-2-butenyl thioethers **2a**–**2c** are interesting in the study of the regioselectitivity of the process of electrophilic cyclization. On one hand, the polarization of the multiple bond of the alkenyl moiety clearly indicates the formation of the thiazine ring via intermediated carbocation, and on the other hand, the high probability of bromonium or iodonium cation formation makes the possibility of the annelation as the five-membered

Scheme 1

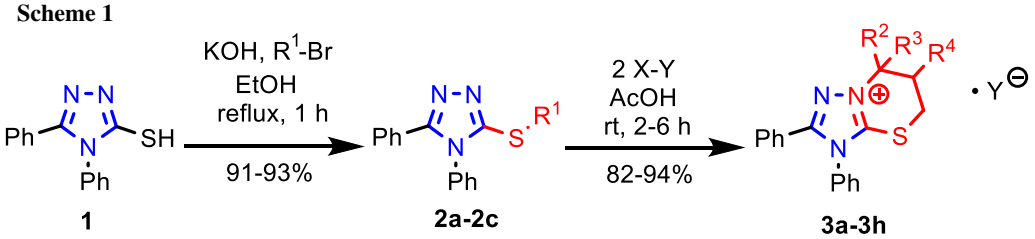

X-Y = Br_2, IBr, I_2

R^1 = (**a**); (**b**); (**c**);

3a: $R^2 = CH_3$; $R^3 = H$; $R^4 = Br$; $Y = Br_3$; **3e:** $R^2 = CH_3$; $R^3 = CH_3$; $R^4 = I$; $Y = Br$;
3b: $R^2 = CH_3$; $R^3 = H$; $R^4 = I$; $Y = Br$; **3f:** $R^2 = CH_2Br$; $R^3 = H$; $R^4 = H$; $Y = Br_3$;
3c: $R^2 = CH_3$; $R^3 = CH_3$; $R^4 = Br$; $Y = Br_3$; **3g:** $R^2 = CH_2I$; $R^3 = H$; $R^4 = H$; $Y = I_3$;
3d: $R^2 = CH_3$; $R^3 = CH_3$; $R^4 = I$; $Y = I_3$; **3h:** $R^2 = CH_2I$; $R^3 = H$; $R^4 = H$; $Y = Br$;

fragment, as well as the thiazine moiety. All abovementioned ways are in the full accordance with modern interpretation of Baldwin rules [29]. The literature contains the information about both direction of electrophilic cyclization in the case of another heterocycles [30–32].

Thus, the comparative analysis of the NMR spectra for the starting thioethers **2** and the halocyclization products **3** shows the change in the nature of the signals of methylene protons, which was observed as doublet at 3.7–3.8 ppm for the parent compounds **2**, and their splitting into two multiplets at 4.0–4.1 ppm for halogenation products **3**. The absence of signals of sp^2-hybritizated carbons of 2-butenyl moiety and the presence of signals of a nodal endocyclic carbon atom in the range of 64.7–67.2 ppm and CH–Hal signal at 40–42 ppm in the ^{13}C NMR spectra of salts **3** also indicate the realization of electrophilic cyclization.

Although the above NMR data were not sufficient for unambiguous structure determination of the received cyclization products **3**, the XDR investigation for salt **3a** has reliably confirmed the structure of bromination product (Fig. 1). From Fig. 1b, it can be seen the presence of Cg1–Cg1 and Cg2–Cg2 interactions that are characterized with the lengths of 4.08 Å and 3.87 Å, respectively.

Experimental data of the XRD investigation for the product of bromocyclization **3a** were used to carry out DFT calculations of the energy profile of the proposed electrophilic cyclization pathway. The comparison of chosen experimental and theoretically calculated bond lengths is presented in Table 2. With respect to reference to know experimental

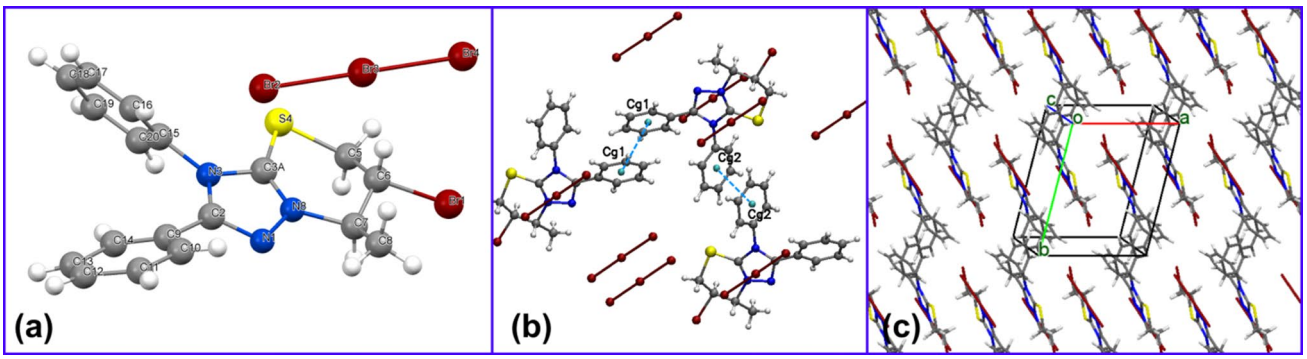

Fig. 1 XRD study of compound **3a**: **a** the structure of the tribromide molecule; **b** Cg–Cg interactions; **c** crystal packing

Table 2 Selected bond lengths of XRD and B3LYP-D3BJ/ma-def2-TZVP geometries of cation **3a** and similar experimental data (in Å)

Bond	Exp	Calc	Lit	Bond	Exp	Calc	Lit
N1–C2	1.34(2)	1.297	1.335 (5) [18] 1.333 (8) [24] 1.299 (3) [26] 1.305 (6) [33]	S4–C5	1.87(2)	1.832	1.850 (4) [18] 1.862 (8) [24] 1.790 (4) [26] 1.788 (5) [33]
C2–N3	1.37(3)	1.368	1.336 (6) [18] 1.372 (9) [24] 1.375 (3) [26] 1.349 (6) [33]	C5–C6	1.42(3)	1.516	1.509 (6) [18]
N3–C3A	1.40(3)	1.346	1.377 (5) [18] 1.315 (8) [24] 1.366 (3) [26] 1.377 (5) [33]	C6–C7	1.41(3)	1.533	1.506 (6) [18]
C3A–N8	1.26(3)	1.333	1.284 (6) [18] 1.323 (9) [24] 1.298 (3) [26] 1.290 (6) [33]	C7–N8	1.56(3)	1.480	1.451 (6) [18] 1.470 (8) [24]
N1–N8	1.40(3)	1.370	1.395 (5) [18] 1.341 (8) [24] 1.398 (3) [26] 1.384 (5) [33]	C7–C8	1.51(3)	1.521	
C3A–S4	1.71(3)	1.718	1.738 (5) [18] 1.680 (6) [24] 1.745 (3) [26] 1.727 (5) [33]	C6–Br1	1.92(2)	1.973	1.964 (5) [18] 1.877 (7) [24] 1.973 (2) [26]

data, we have also included corresponding bond lengths of similar triazolium-containing heterocyclic systems [18, 24, 26, 33]. Calculated interatomic distances are in good agreement with XRD study and mentioned literature data.

DFT calculations

To understand the mechanism of the regioselective halogen-cyclization of considered triazoles **3a–3c,** we have performed a computational study using density functional theory (DFT) methods (see computational methods in the Experimental Section). We will discuss data obtained at B3LYP-D3BJ/ma-def2-TZVP level. In this section, we have considered two model triazoles: 3-(but-2-enyl)thio-4*H*-1,2,4-triazole (**A**) and 3-(3-methylbut-2-enyl)thio-4*H*-1,2,4-triazole (**B**). The substitution of different groups in 4th and 5th positions with hydrogen atoms in the triazole system is valid for reducing the computational resources and must not considerably influence the result, as it was experimentally proven that the regioselectivity of such halogen-cyclization is not controlled by substituents in 4th and 5th positions [28].

Analysis of literature data [11, 12, 18, 27] shows that halogen-mediated hetero-cyclization reactions take place through a two-step mechanism. In a similar way, we have considered processes presented here. At first, the bromine molecule as electrophile attacks on the double bond of the unsaturated fragment to yield molecular complexes **A1**, **A2**, **B1**, and **B2**. Next, molecular complexes form the tri-membered cyclic bromonium cations the bromonium cation immediately attacks the highly nucleophilic N2 nitrogen of the triazole ring in the S_N2-substitution manner yielding the 1,3-thiazenine (**P-A-1**, **P-B-1**) or 1,3-thiazoline (**P-A-2**, **P-B-2**) rings (Scheme 2).

Finally, as the reaction is taken in solution, it is reasonable to consider dissociation of salt-like products to condensed cation and tribromide anion (**S-A/B-1/2**). In general, we have considered bromination through the two regioisomeric channels. Relative Gibbs free energy differences in the acetic acid solution (SMD approach) are given in Table 3.

The reaction starts with the formation of molecular complexes (**A/B-1/2**) between bromine and the π-system of the double bond of unsaturated thioether. According to B3LYP calculations, these complexes are for 41.7/46.8 kJ/mol higher in energy than separated reagents. The activation energies associated with the bonding of Br with the C1 or C2 carbon atoms and the next simultaneous electrophilic attack of the N2 atom, in the case of *S*-but-2-enyl ether is of 12.0 kJ/mol (**TS-A-1**) and 21.6 kJ/mol (**TS-A-2**), whereas in the case of *S*-methallyl ether, the activation energies are of only 0.7 kJ/mol (**TS-B-1**) and 11.9 kJ/mol (**TS-B-2**).

The formation of the corresponding cyclic cations is exothermic by − 154.5, − 189.2, − 61.6, and − 151.1 kJ/mol in

scheme 2

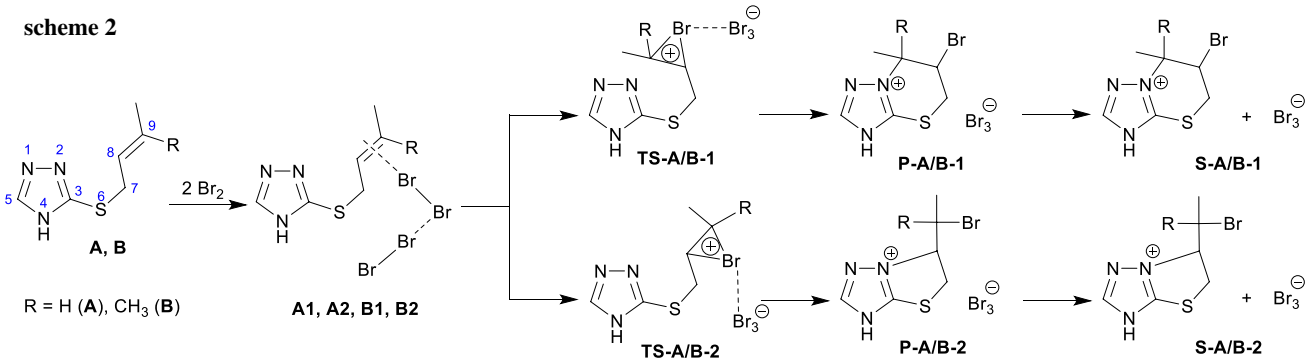

Table 3 Relative Gibbs free energy (in kJ/mol, relative to **A** or **B** plus two bromine molecules) of the stationary points involved in the halogen-cyclization of corresponding triazoles **A** or **B**

Structure	1	2	3	Structure	1	2	3
A1	41.7	65.5	75.2	P-A-1	− 100.8	− 133.7	− 115.5
A2	41.6	65.3	74.9	P-A-2	− 126.0	− 109.1	− 93.2
B1	46.8	72.4	84.9	P-B-1	− 14.1	− 95.5	− 71.5
B2	46.7	72.4	84.9	P-B-2	− 92.5	− 101.9	− 82.3
TS-A-1	53.7	90.4	110.5	S-A-1	− 29.8	− 96.7	− 79.7
TS-A-2	63.2	96.3	119.7	S-A-2	− 86.6	− 38.3	− 23.9
TS-B-1	47.5	80.6	100.6	S-B-1	− 76.7	− 89.2	− 69.3
TS-B-2	58.6	84.0	111.2	S-B-2	− 56.1	− 67.6	− 49.3

Solvation effects of acetic acid were modeled with SMD approach. Used methods are: 1—B3LYP-D3BJ/ma-def2-TZVP; 2—M06-2X/6-311 + G(d,p); 3—ωB97X-D3/6-311 + G(d,p)

the case of **P-A-1**, **P-A-2**, **P-B-1**, and **P-B-2**, respectively. The considerable difference in the case of **P-B-1** structure is due to slightly different orientation of tribromide anion. Thus, in **P-B-1**, the Br_3^- anion coordinated with hydrogens of two methyl groups, whereas in other cases, the IRC procedure leads to structures, where Br_3^- coordinated over the thiazolo-triazole plane, similar to XRD data. These different coordinations do not due to some inconsistence in calculation or wrong theoretical method, this only means that different coordinations of Br_3^- can considerably affect the reaction energy; therefore, in polar solvents, we do have to consider dissociation. Taking into account the above, the Gibbs free energy of dissociation of products with the formation of the cyclic cations and separate tribromide anion is of 71.0, 39.4, − 62.6, and 36.4 kJ/mol in the case of **S-A-1**, **S-A-2**, **S-B-1**, and **S-B-2**, respectively. From these Gibbs free energy calculations, we have to make few important statements: (a) the endothermic bromine attack on the thioether double bond is not regioselective and do not determine the next Br–C bond formation; (b) in both butenyl and isopentenyl thioethers, **TS-A/B-1** transition state is preferable for 9.5/11.1 kJ/mol than **TS-A/B-2**; and (c) the exothermic effect of the cyclization step is higher in the case of six-membered cycle formation (path 1). Consequently, the formation of thiazine ring is kinetically and thermodynamically preferable over the five-membered ring formation.

The geometries of the transition states involved in the bromocyclization of thioethers **A** and **B** are shown in Fig. 2. In the case of cyclization of thioethers to six-membered cycles, the lengths of the C6-Br13/N5-C11 forming bond are 2.18/2.23 and 2.19/2.37 Å in the **TS-A-1** and **TS-B-1**, respectively, whereas in the case of TSs that lead to five-membered cycles, **TS-A-2** and **TS-B-2**, the lengths of the C11-Br13/N5-C6 forming bond are 2.50/2.30 and 2.15/2.29 Å, respectively.

Conclusion

In conclusion, we have developed an efficient and general way for regio-selective synthesis of partially saturated triazolo[5,1-*b*][1,3]thiazinium salts via an electrophilic heterocyclization strategy using the butenyl thioethers of 4,5-diphenyl-1,2,4-triazol-3-thiol and halogenes. The target condensed products were prepared with high yields under finding reaction conditions: room temperature, stirring, polar solvent, and twice excess of electrophile. The studying of the regiochemistry of this process using computer simulation

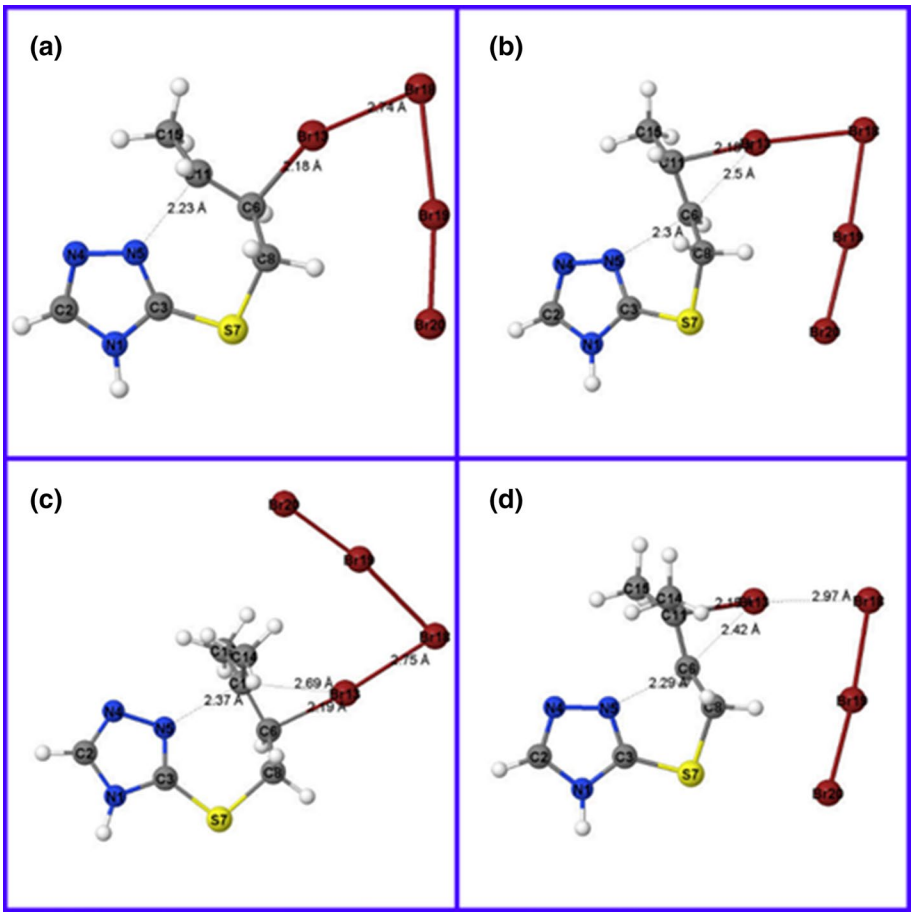

Fig. 2 Geometries of the TSs involved in the bromocyclization: **TS-A-1** (**a**), **TS-A-2** (**b**), **TS-B-1** (**c**), and **TS-B-2** (**d**). The bond lengths are given in Å

methods, XDR, and spectral investigations have been used for explaining of electrophilic cyclization mechanism and reliably solving of target products structure. In view of facile work-up and the easy availability of the starting butenyl thioethers of 4,5-diphenyl-1,2,4-triazol-3-thiol, as well as the broad potential for application of received partially saturated triazolo[5,1-*b*][1,3]thiazines, these protocols should be of great interest in organic chemistry and related disciplines.

Experimental

All reagents were obtained from commercial suppliers and used without any further purification. Solution of iodine bromide (1 mmol/cm^3) was prepared according to standard procedure [34]. The melting points were determined on Stuart SMP30 instrument. ^{1}H NMR (400 MHz) and ^{13}C NMR (100 MHz) spectra were recorded in $(CD_3)_2SO$ as a solvent and TMS as an internal standard on Varian VXR 400. Elemental analyses were performed on Elementar Vario MICRO cube analyzer. All crystallographic measurements were performed at room temperature [293(2) K] on single-crystal diffractometer "Oxford Diffraction Xcalibur".

Starting geometries were modeled in the Avogadro [35] and Gabedit [36] programs. At first, we have and pre-optimized starting structures, transition states (TSs) and cyclized products with fast GGA BLYP functional [37, 38] in combination with 6-311 + G(d,p) basis set [39, 40]. Computed Hessians in the cases of TSs contained only one imaginary frequency. Intrinsic reaction coordinate (IRC) calculations [41] clearly testifies the correctness of founded TSs that correspond to proposed reaction path. Then after, obtained structures were re-optimized at the B3LYP/ma-def2-TZVP level of theory [42–44] supported by D3 dispersion correction [45] in Becke–Johnson damping variant [46]. Moreover, with comparison purpose, we have performed single point energy calculations at M06-2X/6-311 + G(d,p) [47] and ωB97X-D3/6-311 + G(d,p) [48] levels of theory. For taking into account the solvent effect, we have performed single-point computations with using of SMD model [49]. The PRIRODA program was used for BLYP DFT calculations [50]. The ORCA 4 package [51] was used for all calculation conducted with B3LYP method. To reduce the computational time without considerable loss in accuracy, the density fitting technique was used [52–54] with appropriate auxiliary basis set [55]. Visualization of output optimized structures were made using the Jmol program [56].

General procedure for the synthesis of compounds 2

4,5-Diphenyl-2,4-dihydro-3*H*-1,2,4-triazole-3-thione 1 (10.0 mmol) was dissolved in 20 cm^3 ethanol with the addition of potassium hydroxide (12.0 mmol) when heated. The alkenyl bromides (12.0 mmol) in 5 cm^3 ethanol were added to the cooled solution of triazole **1**. The mixture was boiled for 1 h. After cooling, the precipitated product was filtered, washed with deionized water, and purified by crystallization from ethanol.

3-[(2*E*)-But-2-en-1-ylsulfanyl]-4,5-diphenyl-4*H*-1,2,4-triazole (2a, $C_{18}H_{17}N_3S$) Yield 92%; white powder; m.p.: 137–139 °C; FT-IR: $\bar{\nu}$ = 1610 (C=N), 1530 (C=C, Ph), 1425 (C=C, Ph), 1230 (=C–N <), 1130 (> C–C=), 775 (C-S) cm^{-1}; ^{1}H NMR (400 MHz, DMSO-d_6): δ = 7.29–7.60 (10H, m, 2 C_6H_5), 5.64–5.70 (1H, m, = CH), 5.43-5.59 (1H, m, = CH), 3.77 (2H, dd, J = 28.6, 7.1 Hz, CH_2), 1.61 (3H, s, CH_3) ppm; ^{13}C NMR (100 MHz, DMSO-d_6): δ = 154.7 (C^5=N), 151.91 (C^3=N), 134.3 (C, 4-Ph), 130.4 (2C^{m}H, 4-Ph), 130.1 (C^{p}H, 5-Ph), 129.8 (=*C*H–CH_3), 129.2 (2C^{m}H, 5-Ph), 129.0 (2C^{o}H, 5-Ph), 128.8 (C^{p}H, 4-Ph), 128.2 (2C^{o}H, 4-Ph), 127.09 (CH_2–*C*H=), 126.2 (C, 5-Ph), 34.8 (CH_2), 18.0 (CH_3) ppm.

3-[(3-Methylbut-2-en-1-yl)sulfanyl]-4,5-diphenyl-4*H*-1,2,4-triazole (2b, $C_{19}H_{19}N_3S$) Yield 91%; white powder; m.p.: 136–137 °C; FT-IR: $\bar{\nu}$ = 1600 (C=N), 1530 (C=C, Ph), 1430 (C=C, Ph), 1230 (=C–N <), 1125 (> C–C=), 775 (C-S) cm^{-1}; ^{1}H NMR (400 MHz, DMSO-d_6): δ = 7.34–7.52 (10H, m, 2 C_6H_5), 5.28 (1H, J = 9.2 Hz, CH), 3.77 (2H, d, J = 9.2 Hz, CH_2), 1.64 (3H, s, CH_3), 1.58 (3H, s, CH_3) ppm.

3-(But-3-en-1-ylsulfanyl)-4,5-diphenyl-4*H*-1,2,4-triazole (2c, $C_{18}H_{17}N_3S$) Yield 93%; white powder; m.p.: 133–135 °C; FT-IR: $\bar{\nu}$ = 1600 (C=N), 1530 (C=C, Ph), 1425 (C=C, Ph), 1235 (=C–N <), 1125 (> C–C=), 770 (C-S) cm^{-1}; ^{1}H NMR (400 MHz, DMSO-d_6): δ = 7.49–7.58 (3H, m, C_6H_5), 7.27–7.44 (7H, m, C_6H_5), 5.79 (1H, dt, J = 16.9, 10.3, 6.6 Hz, CH), 4.98–5.14 (2H, m, = CH_2), 3.22 (2H, t, J = 7.2 Hz, CH_2), 2.45 (2H, d, J = 7.1 Hz, CH_2) ppm; ^{13}C NMR (100 MHz, DMSO-d_6): δ = 154.8 (C^5=N), 152.3 (C^3=N), 136.6 (C, 4-Ph), 134.4 (C^{p}H, 5-Ph), 130.5 (2C^{m}H, 4-Ph), 130.4 (2C^{m}H, 5-Ph), 130.2, (2C^{o}H, 5-Ph), 129.0 (C^{p}H, 4-Ph), 128.3 (2C^{o}H, 4-Ph), 128.2 (C, 5-Ph), 127.1 (CH_2–*C*H=), 117.1 (=CH_2), 33.5 (SCH_2), 31.7 (*C*H_2CH=) ppm.

General procedure for the synthesis of compounds 3

The solution of appropriated halogen (2.0 mmol) in acetic acid was dropwise added to the solution of triazoles **2** (1.0 mmol) in acetic acid with constant stirring at room temperature. The reaction mixture was stirred at room temperature for 2–6 h; the product was filtered and washed with acetic acid.

6-Bromo-7-methyl-2,3-diphenyl-3,5,6,7-tetrahydro[1,2,4]-triazolo[5,1-*b*][1,3]thiazine-8-ium tribromide (3a, $C_{18}H_{17}Br_4N_3S$) Yield 82%; orange powder; m.p.: 152 °C; FT-IR: $\bar{\nu}$ = 1530 (C=C, Ph), 1475 (C=N$^+$), 1425 (C=C, Ph), 1375 (C–CH_3), 1240 (=C–N<), 770 (C–S), 690 (C–Br) cm^{-1}; ^{1}H NMR (400 MHz, DMSO-d_6): δ = 7.32–7.84 (10H, m, 2 C_6H_5), 5.02–5.34 (2H, m, +NCH, CHBr), 4.08 (1H, dd, J = 8.2 Hz, 2.7 Hz, SCH_2), 3.75–3.93 (1H, m, SCH_2), 1.76 (3H, s, CH_3) ppm; ^{13}C NMR (100 MHz, DMSO-d_6): δ = 152.4 (C^3=N$^+$), 151.3 (C^5=N), 132.0 (C, 4-Ph), 131.7 (C^pH, 5-Ph; 2C^mH, 5-Ph; 2C^mH, 4-Ph), 130.6 (2C^oH, 5-Ph), 128.9 (C^pH, 4-Ph), 127.4 (2C^oH, 4-Ph), 122.6 (C, 5-Ph), 62.2 (CHN$^+$), 44.4 (CHBr), 31.8 (CH_2), 19.7 (CH_3) ppm; UV (C_2H_5OH): λ_{max} = 262 nm.

CCDC 1,878,957. X-ray study was carried out using «Xcalibur-3» automated diffractometer (Oxford Diffraction Ltd.) (MoKα-radiation, graphite monochromator, «Sapphire-3» CCD detector. The structure was solved with SHELX-2014/7 program package [57] and refined using full-matrix least squares in the anisotropic approximation. Hydrogen atoms were added geometrically and refined using the «riding model». The WinGX program [58] was used for the analysis of the structure and preparation of illustration.

6-Iodo-7-methyl-2,3-diphenyl-3,5,6,7-tetrahydro[1,2,4]-triazolo[5,1-*b*][1,3]thiazine-8-ium bromide (3b, $C_{18}H_{17}BrIN_3S$) Yield 94%; yellowish powder; m.p.: 147 °C; FT-IR: $\bar{\nu}$ = 1530 (C=C, Ph), 1480 (C=N$^+$), 1430 (C=C, Ph), 1375 (C–CH_3), 1255 (=C–N<), 775 (C–S), 580 (C–I) cm^{-1}; ^{1}H NMR (400 MHz, DMSO-d_6): δ = 7.38–7.80 (10H, m, 2 C_6H_5), 4.98–5.11 (2H, m, +NCH, CHI), 3.97 (1H, d, J = 13.5 Hz, SCH_2), 3.84 (1H, d, J = 7.9 Hz, SCH_2), 1.80 (3H, s, CH_3) ppm; ^{13}C NMR (100 MHz, DMSO-d_6): δ = 152.6 (C^3=N$^+$), 151.9 (C^5=N), 132.6 (C, 4-Ph), 131.3 (C^pH, 5-Ph; 2C^mH, 5-Ph; 2C^mH, 4-Ph), 129.6 (2C^oH, 5-Ph), 129.3 (C^pH, 4-Ph), 127.8 (2C^oH, 4-Ph), 123.0 (C, 5-Ph), 63.8 (CHN$^+$), 34.0 (CH_2), 20.8 (CHI), 20.3 (CH_3) ppm; UV (C_2H_5OH): λ_{max} = 264 nm.

6-Bromo-7,7-dimethyl-2,3-diphenyl-3,5,6,7-tetrahydro-[1,2,4]triazolo[5,1-*b*][1,3]thiazine-8-ium tribromide (3c, $C_{19}H_{19}Br_4N_3S$) Yield 84%; orange powder; m.p.: 158–159 °C; FT-IR: $\bar{\nu}$ = 1530 (C=C, Ph), 1480 (C=N$^+$), 1430 (C=C, Ph), 1385 [$C(CH_3)_2$], 1240 (=C–N<), 770 (C–S), 700 (C–Br) cm^{-1}; ^{1}H NMR (400 MHz, DMSO-d_6): δ = 7.35–7.81 (10H, m, 2 C_6H_5), 5.09–5.23 (1H, m, CHI), 3.86-4.23 (2H, m, SCH_2), 1.92 (3H, s, CH_3), 1.86 (3H, s, CH_3) ppm; UV (C_2H_5OH): λ_{max} = 264 nm.

6-Iodo-7,7-dimethyl-2,3-diphenyl-3,5,6,7-tetrahydro-[1,2,4]triazolo[5,1-*b*][1,3]thiazine-8-ium triiodide (3d, $C_{19}H_{19}I_4N_3S$) Yield 86%; brown powder; m.p.: 152–153 °C; FT-IR: $\bar{\nu}$ = 1530 (C=C, Ph), 1480 (C=N$^+$), 1430 (C=C, Ph), 1385 [$C(CH_3)_2$], 1255 (=C–N<), 775 (C–S), 590 (C–I) cm^{-1}; ^{1}H NMR (400 MHz, DMSO-d_6): δ = 7.42–7.63 (10H, m, 2 C_6H_5), 5.10–5.18 (1H, m, CHI), 4.10 (1H, d, J = 3.4 Hz, SCH_2), 3.88-4.07 (1H, m, SCH_2), 1.92 (3H, s, CH_3), 1.89 (3H, s, CH_3) ppm; ^{13}C NMR (100 MHz, DMSO-d_6): δ = 152.4 (C^3=N$^+$), 151.8 (C^5=N), 132.6 (C, 4-Ph), 132.5 (C^pH, 5-Ph), 131.3 (2C^mH, 5-Ph), 131.1 (2C^mH, 4-Ph), 129.6 (2C^oH, 5-Ph), 129.3 (C^pH, 4-Ph), 127.8 (2C^oH, 4-Ph), 123.1 (C, 5-Ph), 65.2 (CHN$^+$), 33.5 (CH_2), 28.7 (CHI), 28.1 (CH_3), 27.7 (CH_3) ppm; UV (C_2H_5OH): λ_{max} = 252 nm.

6-Iodo-7,7-dimethyl-2,3-diphenyl-3,5,6,7-tetrahydro-[1,2,4]triazolo[5,1-*b*][1,3]thiazine-8-ium bromide (3e, $C_{19}H_{19}BrIN_3S$) Yield 84%; yellowish powder; m.p.: 158–159 °C; FT-IR: $\bar{\nu}$ = 1530 (C=C, Ph), 1480 (C=N$^+$), 1430 (C=C, Ph), 1375 [$C(CH_3)_2$], 1255 (=C–N<), 775 (C–S), 590 (C–I) cm^{-1}; ^{1}H NMR (400 MHz, DMSO-d_6): δ = 7.35–7.81 (10H, m, 2 C_6H_5), 5.09–5.23 (1H, m, CHI), 3.86-4.23 (2H, m, SCH_2), 1.92 (3H, s, CH_3), 1.86 (3H, s, CH_3) ppm; ^{13}C NMR (100 MHz, DMSO-d_6): δ = 151.8 (C^3=N$^+$), 151.4 (C^5=N), 131.9 (C, 4-Ph), 131.0 (C^pH, 5-Ph), 130.6 (2C^mH, 5-Ph), 130.1 (2C^mH, 4-Ph), 128.9 (2C^oH, 5-Ph), 128.6 (C^pH, 4-Ph), 127.5 (2C^oH, 4-Ph), 122.7 (C, 5-Ph), 64.7 (CHN$^+$), 33.0 (CH_2), 28.2 (CHI), 27.4 (CH_3), 27.3 (CH_3) ppm; UV (C_2H_5OH): λ_{max} = 252 nm.

7-(Bromomethyl)-2,3-diphenyl-3,5,6,7-tetrahydro[1,2,4]-triazolo[5,1-*b*][1,3]thiazine-8-ium tribromide (3f, $C_{18}H_{17}Br_4N_3S$) Yield 88%; orange powder; m.p.: 167–168 °C; FT-IR: $\bar{\nu}$ = 1530 (C=C, Ph), 1475 (C=N$^+$), 1430 (C=C, Ph), 1240 (=C–N<), 770 (C–S), 735 (C–Br) cm^{-1}; ^{1}H NMR (400 MHz, DMSO-d_6): δ = 7.24–7.57 (10H, m, 2 C_6H_5), 4.99–5.07 (2H, m, +NCH, CH_2Br), 4.19–4.27 (1H, m, CH_2Br), 3.86–3.96 (1H, m, SCH_2), 3.59 (1H, m, SCH_2), 3.20 (1H, t, J = 7.2 Hz, CH_2), 2.72 (1H, d, J = 7.0 Hz, CH_2) ppm; UV (C_2H_5OH): λ_{max} = 263 nm.

7-(Iodomethyl)-2,3-diphenyl-3,5,6,7-tetrahydro[1,2,4]-triazolo[5,1-*b*][1,3]thiazine-8-ium triiodide (3g, $C_{18}H_{17}I_4N_3S$) Yield 84%; brown powder; m.p.: 173–175 °C; FT-IR: $\bar{\nu}$ = 1530 (C=C, Ph), 1475 (C=N$^+$), 1455 (C=C, Ph), 1250 (=C–N<), 775 (C–S), 610 (C-I) cm^{-1}; ^{1}H NMR (400 MHz, DMSO-d_6): δ = 7.31–7.71 (10H, m, 2 C_6H_5), 4.97–5.16 (1H, m, +NCH, CH_2I), 3.55 (1H, dd, J = 6.5, 4.7 Hz, CH_2I), 3.23 (2H, dd, J = 13.5, 5.7 Hz, SCH_2), 2.38–2.52 (2H, m, CH_2) ppm; ^{13}C NMR (100 MHz, DMSO-d_6): δ = 154.8 (C^3=N$^+$), 153.2 (C^5=N), 132.6 (C, 4-Ph), 131.1 (C^pH, 5-Ph), 130.0 (2C^mH, 5-Ph), 129.0 (2C^mH, 4-Ph), 128.4 (2C^oH, 5-Ph), 128.2 (C^pH, 4-Ph), 127.9 (2C^oH, 4-Ph), 117.2 (C, 5-Ph), 59.1 (CHN$^+$), 33.5 (CH*C*H$_2$), 31.7 (SCH_2), 26.9 (CH_2I) ppm; UV (C_2H_5OH): λ_{max} = 260 nm.

7-(Iodomethyl)-2,3-diphenyl-3,5,6,7-tetrahydro[1,2,4]-triazolo[5,1-*b*][1,3]thiazine-8-ium bromide (3h, $C_{18}H_{17}BrIN_3S$) Yield 82%; yellowish powder; m.p.: 167–169 °C; FT-IR: $\bar{\nu}=1530$ (C=C, Ph), 1475 (C=N$^+$), 1450 (C=C, Ph), 1255 (=C–N<), 775 (C–S), 610 (C–I) cm^{-1}; ^{1}H NMR (400 MHz, DMSO-d_6): $\delta=7.28$–7.78 (10H, m, 2 C_6H_5), 5.04 (2H, d, $J=22.0$ Hz, CH_2I), 4.12–4.30 (1H, m, CH), 3.83–4.01 (1H, m, SCH_2), 3.61 (1H, s, SCH_2), 3.09–3.23 (1H, m, CH_2), 2.70 (1H, s, CH_2) ppm; UV (C_2H_5OH): $\lambda_{max}=260$ nm.

Acknowledgements This work was supported by the Ministry of Education and Science of Ukraine (Project GR-0119U100232).

References

1. Danilkina M, Vershilov S, Ganina M, Mikhailov L, Ivin B (2004) Russ J Gen Chem 74:472
2. Britsun V, Esipenko A, Kudryavtsev A, Lozinskii M (2004) Russ J Org Chem 40:232
3. Britsun V, Lozinskii M (2004) Chem Heterocycl Compd 40:1092
4. Motamedi R, Heravi M, Nazari Z, Bamoharram F (2010) Phosphorus Sulfur Silicon Relat Elem 185:1672
5. Slivka M, Korol N, Rusyn I, Lendel V (2015) Heterocycl Commun 21:397
6. Tozkoparan B, Aktay G, Yeşilada E (2002) Farmaco 57:145
7. Foks H, Rudnicca W, Glowka M, Kaliszan R, Nasal A, Damasiewicz B, Radwanska A, Petrusewicz J, Trzeciak H, Okopien B (1992) Pharmazie 47:770
8. Lal Dhar SY, Misra AR, Singh H (1988) J Agric Food Chem 36:626
9. Kut M, Onysko M, Lendel V (2016) Heterocycl Commun 22:347
10. Slivka M, Krivovjaz A, Slivka M, Lendel V (2013) Heterocycl Commun 19:189
11. Korol N, Slivka M (2017) Chem Heterocycl Compd 53:852
12. Kochikyan T, Samvelyan M, Petrosyan A, Langer P (2015) Russ J Org Chem 51:1469
13. Khripak S, Slivka M, Vilkov R, Usenko R, Lendel V (2007) Chem Heterocycl Compd 43:781
14. Slivka M, Khripak S, Britsun V, Staninets V (2000) Russ J Org Chem 36:1033
15. Dyachenko I, Vas'kevich R, Vas'kevich A, Shishkina S, Vovk M (2016) Russ J Org Chem 52:755
16. Onysko M, Filak I, Lendel V (2016) Heterocycl Commun 22:295
17. Fizer M, Slivka M (2016) Chem Heterocycl Compd 52:155
18. Fizer M, Slivka M, Rusanov E, Turov A, Lendel V (2015) J Heterocycl Chem 52:949
19. Vaskevich R, Vaskevich A, Turov A, Staninets V, Vovk M (2011) Chem Heterocycl Compd 47:1037
20. Tarasova N, Kim D, Eltsov O, Shtukina T, Borisov A (2018) Russ J Org Chem 54:469
21. Fizer MM, Slivka MV, Lendel VG (2019) Chem Heterocycl Compd 55:478
22. Yushina I, Tarasova N, Kim D, Sharutin V, Bartashevich E (2019) Crystals 9:506
23. Danyliuk IYu, Vas'kevich RI, Vas'kevich AI, Rusanov EB, Vovk MV (2019) Phosphorus Sulfur Silicon Relat Elem 194:156
24. Slivka M, Korol N, Pantyo V, Baumer V, Lendel V (2017) Heterocycl Commun 23:109
25. Usenko R, Slivka M, Lendel V (2011) Chem Heterocycl Compd 47:1029
26. Slivka M, Korol N, Fizer M, Baumer V, Lendel V (2018) Heterocycl Comm 24:197
27. Shmygarev V, Kim D (2004) Chem Heterocycl Compd 40:1207
28. Ilinykh E, Kim D, Kodess M, Matochkina E, Slepukhin P (2013) J Fluorine Chem 149:24
29. Gilmore K, Alabugin IV (2011) Chem Rev 111:6513
30. Kim D, Sudolova N, Slepukhin P, Charushin V (2011) Chem Heterocycl Compd 46:1420
31. Onysko M, Filak I, Lendel V (2017) Heterocycl Commun 23:309
32. Rybakova A, Kim D, Ezhikova M, Kodess M, Taher I (2015) Russ Chem Bull 64:901
33. Fizer M, Slivka M, Mariychuk R, Baumer V, Lendel V (2018) J Mol Struct 1161:226
34. Brisbois RG, Wanke RA, Field RA, Mukhopadhyay B, Korol N, Slivka M (2018) Iodine Monobromide. Encyclopedia of reagents for organic synthesis. Wiley, New York
35. Hanwell MD, Curtis DE, Lonie DC, Vandermeersch T, Zurek E, Hutchison GR (2012) J Cheminf 4:17
36. Allouche AR (2011) J Comput Chem 32:174
37. Becke AD (1988) Phys Rev A: At Mol Opt Phys 38:3098
38. Lee C, Yang W, Parr RG (1988) Phys Rev B: Condens Matter 37:785
39. Krishnan R, Binkley JS, Seeger R, Pople JA (1980) J Chem Phys 72:650
40. Clark T, Chandrasekhar J, Spitznagel GW, Schleyer PVR (1983) J Comput Chem 4:294
41. Maeda S, Harabuchi Y, Ono Y, Taketsugu T, Morokuma K (2015) Int J Quantum Chem 115:258
42. Becke AD (1993) J Chem Phys 98:5648
43. Weigend F, Ahlrichs R (2005) Phys Chem Chem Phys 7:3297
44. Zheng J, Xu X, Truhlar XG (2011) Theor Chem Acc 128:295
45. Grimme S, Antony J, Ehrlich S, Krieg H (2010) J Chem Phys 132:154104
46. Grimme S, Ehrlich S, Goerigk L (2011) J Comput Chem 32:1456
47. Zhao Y, Truhlar DG (2006) Theor Chem Acc 120:215
48. Lin YS, Li GD, Mao SP, Chai JD (2013) J Chem Theory Comput 9:263
49. Marenich AV, Truhlar DG (2009) J Phys Chem B 113:6378
50. Laikov DN, Ustynyuk AYu (2005) Russ Chem Bull 54:820
51. Neese F (2018) Comput Mol Sci 8:e1327
52. Laikov DN (1997) Chem Phys Lett 281:151
53. Neese F (2003) J Comput Chem 24:1740
54. Neese F, Wennmohs F, Hansen A, Becker U (2009) Chem Phys 356:98
55. Stoychev GL, Auer AA, Neese F (2017) J Chem Theory Comput 13:554
56. Jmol: an open-source Java viewer for chemical structures in 3D. http://www.jmol.org/. Accessed 20 May 2019
57. Sheldrick GM (2015) Acta Cryst C 71:3
58. Farrugia LJ (1999) J Appl Cryst 32:837